Original Article

Relationship between freezing of gait in Parkinson disease and locus coeruleus dysfunction: a neuromelanin-sensitive magnetic resonance imaging study

Yanyan Yang[1], Mengchao Zhang[1], Yayun Yan[2], Ying Chang[2], Mingxin Chen[3]

[1]Department of Radiology, China-Japan Union Hospital of Jilin University, Changchun, China; [2]Department of Neurology, China-Japan Union Hospital of Jilin University, Changchun, China; [3]Emergency and Outpatient Department, China-Japan Union Hospital of Jilin University, Changchun, China

Contributions: (I) Conception and design: Y Yang, M Zhang, M Chen; (II) Administrative support: M Zhang, M Chen; (III) Provision of study materials or patients: Y Yan, Y Chang; (IV) Collection and assembly of data: Y Yang, Y Yan, M Chen; (V) Data analysis and interpretation: Y Yang, M Zhang, Y Yan; (VI) Manuscript writing: All authors; (VII) Final approval of manuscript: All authors.

Correspondence to: Mingxin Chen, MD. Emergency and Outpatient Department, China-Japan Union Hospital of Jilin University, Sendai Dajie, Changchun 130000, China. Email: chenmingxin@jlu.edu.cn.

Background: Preliminary scientific evidence suggests that freezing of gait (FoG) in patients with Parkinson disease (PD) is linked to noradrenergic dysfunction in the locus coeruleus (LC). However, definitive findings regarding the correlation between FoG occurrence and the LC are lacking. This study thus aimed to investigate the relationship between the FoG occurrence and LC degeneration in patients with PD by analyzing the signal characteristics of the LC in neuromelanin-sensitive magnetic resonance imaging (NM-MRI).

Methods: This study enrolled 22 patients with PD and FoG, 24 patients with PD without FoG, and 13 matched healthy controls (HCs). All participants underwent magnetic resonance imaging (MRI) scanning and clinical assessments. The contrast-to-noise ratio (CNR) of LC was measured on NM-MRI images. We used two statistical models (model 1 and model 2) to screen and adjust for potential confounding factors and evaluated the independent relationship between LC's CNR and FoG.

Results: The statistical models showed that except for the target factor FoG [model 1: β=0.127, 95% confidence interval (CI): 0.019–0.236, P=0.023; model 2: β=0.153, 95% CI: 0.019–0.287, P=0.026], rapid-eye-movement sleep behavior disorder (RBD) (model 1: β=0.182, 95% CI: 0.073–0.291, P=0.002; model 2: β=0.171, 95% CI: 0.048–0.294, P=0.008), and gender (model 1: β=0.150, 95% CI: 0.042–0.257, P=0.007) were independent factors associated with the CNR of the left LC. Among these, RBD had the greatest influence, followed by gender and FoG.

Conclusions: Our findings indicated that the FoG is associated with noradrenergic dysfunction caused by LC degeneration.

Keywords: Parkinson disease (PD); freezing of gait (FoG); neuromelanin-sensitive magnetic resonance imaging (NM-MRI); locus coeruleus (LC)

Submitted Jul 22, 2024. Accepted for publication Dec 05, 2024. Published online Dec 17, 2024.
doi: 10.21037/qims-24-1486
View this article at: https://dx.doi.org/10.21037/qims-24-1486

Introduction

Freezing of gait (FoG) is a common gait pattern in individuals with advanced Parkinson disease (PD) with a poor prognosis and significantly affects patients' quality of life in terms of falls and disability (1). However, the pathophysiological mechanism underlying the emergence of FoG in PD is still unclear.

Nondopaminergic pathways are assumed to be involved in FoG occurrence since they are in an "on" state but do not respond adequately to dopamine replacement therapy or deep brain stimulation (2,3). Dysfunction of the noradrenergic network in FoG has been confirmed in analyses on behavioral characteristics and some pharmacological and laboratory evidence. Behavioral studies suggest that FoG is often triggered by impaired attention and executive function during the approach to a destination and performance of dual tasks, which is often accompanied by noradrenergic dysfunction (4,5). Extensive pharmacological evidence suggests that certain norepinephrine (NE) prodrugs can improve FoG symptoms; however, there may be variability in efficacy because these drugs tend to be effective in patients with dopamine resistance or those with advanced-stage FoG (6). In addition, a laboratory examination with a small sample of cerebrospinal fluid revealed that the concentration of NE decreases significantly with the progression of FoG (7,8).

Neuromelanin-sensitive magnetic resonance imaging (NM-MRI), a novel magnetic resonance imaging (MRI) technique, is purportedly capable of indirectly assessing the noradrenergic function of the locus coeruleus (LC) (9-12), which is the main noradrenergic nucleus of the brain and serves as the largest "reservoir" of NE *in vivo* (13). Large-sample NM-MRI studies of the LC in patients with PD have identified a positive correlation between LC degeneration and nonmotor symptoms, such as psychiatric alterations, sleep disruption [especially rapid-eye-movement sleep behavior disorder (RBD)], cognitive impairment, depression, and apathy (14-16). In addition, these nonmotor symptoms have been found to be some of the risk factors for FoG (17,18), which has prompted researchers to investigate the relationship between FoG and LC degeneration in PD via NM-MRI.

We therefore posited the following hypothesis: LC degeneration in PD is independently associated with FoG occurrence. This study aimed to investigate the relationship between LC NM-MRI features—which can reflect the function of NE—and FoG occurrence. We employed a retrospective approach and due to the presence of numerous confounding factors influencing LC NM-MRI features, we used two statistical models, multifactor stepwise linear regression and the change-in-estimate (CIE) method, to screen and adjust for these factors; thus, we could determine the independent relationship between LC NM-MRI features and FoG. We present this article in accordance with the STROBE reporting checklist (available at https://qims.amegroups.com/article/view/10.21037/qims-24-1486/rc).

Methods

Participants

From March 2022 to December 2022, we consecutively reviewed 70 patients with PD and 15 healthy controls (HCs) from the Department of Neurology, China-Japan Union Hospital of Jilin University, to investigate the LC NM-MRI features. The clinical diagnosis of patients with PD was performed according to the criteria set by the Movement Disorder Society in 2015 (19). The exclusion criteria for patients with PD were as follows: (I) dementia; (II) incomplete responses to the required questionnaires; and (III) poor image quality. Meanwhile, the exclusion criteria for the HC group were (I) a history of severe neurological or psychiatric disorders or neurodegenerative diseases and (II) poor image quality.

We ultimately enrolled 46 patients with PD and 13 HCs: 23 patients were excluded because of incomplete scale information and one patient because of dementia, and two HCs were excluded because of poor scan quality. Patients with PD were divided into the PD FoG+ group (n=22) and the PD FoG– group (n=24). This study was approved by the Ethics Review Committee of the China-Japan Union Hospital of Jilin University (No. 2023111003) and conducted in accordance with the Declaration of Helsinki (as revised in 2013). Informed consent was obtained from all the patients.

Clinical and neuropsychology evaluations

In this study, we aimed to investigate whether FoG is independently associated with the contrast-to-noise ratio (CNR) of the LC. FoG status was defined according to the clinical features assessed by senior physicians who had been working for more than 10 years and a FoG self-report index with a minimum score of 2 on item 3, the Freezing of Gait Questionnaire (FoG-Q) (20). Clinical

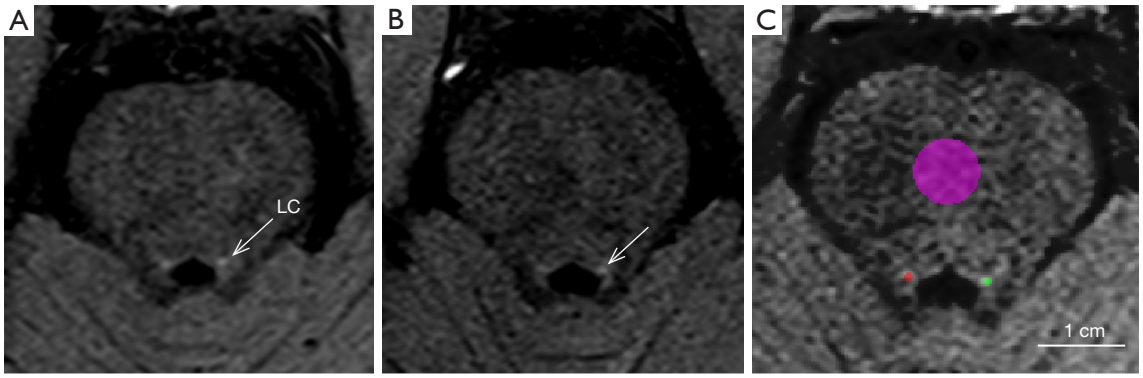

Figure 1 NM-MRI of the LC. (A) The LC in the HC group (white arrow). (B) The LC in the PD group (white arrow). (C) The locations of the LC ROIs (green and red circular ROIs) and PT ROIs (purple circular ROIs) in ITK-SNAP software are shown. LC, locus coeruleus; NM-MRI, neuromelanin-sensitive magnetic resonance imaging; HC, healthy control; PD, Parkinson disease; ROI, region of interest; PT, medial pontine.

features primarily included the following: (I) a foot or toe tip not moving off the ground or only moving across the ground; (II) the legs trembling alternately on both sides at a frequency of 3 to 8 Hz; (III) a feeling of feet being "stuck" to the floor during freezing; and (IV) starting hesitancy, or a sudden inability to lift the feet when turning, during walks through narrow passages or when reaching a destination. Based on previous research, we considered nine potential confounders including age, gender, RBD, disease duration, cognitive impairment, depression, apathy, orthostatic hypotension (OH), and disease severity. Among them, gender, RBD, and OH were binary variables, while age, disease duration, cognitive impairment, depression, apathy, and disease severity were continuous variables. Some of the assessment methods for the confounders are listed below: (I) RBD was determined according to the proportion of Rapid Eye Movement Sleep Behavior Disorder Screening Questionnaire (RBDSQ) items ≥5 points in combination with the patients' chief complaints (21,22); (II) cognitive impairment assessed with the Montreal Cognitive Assessment (MoCA) (23); (III) depression was evaluated via the Hamilton Depression Rating Scale (HAMD) (24); (IV) apathy was measured via the Apathy Scale (AS) (25); (V) OH was determined based on the patient's complaints; and (VI) disease severity was assessed by the Unified Parkinson's Disease Rating Scale III (UPDRS-III) (26).

MRI data acquisition

The imaging data were acquired on a 3-T Tesla MRI scanner (MAGNETOM Skyra, Siemens Healthineers, Erlangen, Germany) with a 16-channel head coil. All participants were given detailed instructions on precautions and were instructed to remain quiet during the scan. In addition, foam pads were used to reduce patient head movement, and earplugs were used to reduce the noise from the scanner.

NM-MRI was performed using two-dimensional (2D) T1-weighted imaging combined with magnetization transfer-weighted MRI. The relevant parameters were as follows: time to repetition/time to echo (TR/TE), 887/15 ms; echo train length, 2; section thickness, 2.5 mm with no intersection gap; slice number, 16; matrix size, 448×291; field of view, 220 mm; number of excitations, 7; and acquisition time, 7 minutes and 34 seconds. The scout image was set parallel to the anterior and posterior commissure of the corpus callosum in the axial view, covering the posterior commissure to the pons. The scanning range was from the upper basal ganglia to the lower medulla oblongata. In addition, routine cranial MRI scan sequences were obtained to exclude pathological brain changes that might interfere with imaging evaluation.

NM-MRI image processing

We used ITK-SNAP software to make two artificial image measurements (27). The intraclass correlation coefficient for the interrater agreement was 0.827. The LC is a roughly cylindrical, hyperpigmented nucleus in the cephalic pons adjacent to the fourth ventricle and above the pontomedullary junction (28). Representative NM-MRI images of the LC are shown in *Figure 1A,1B*. We defined

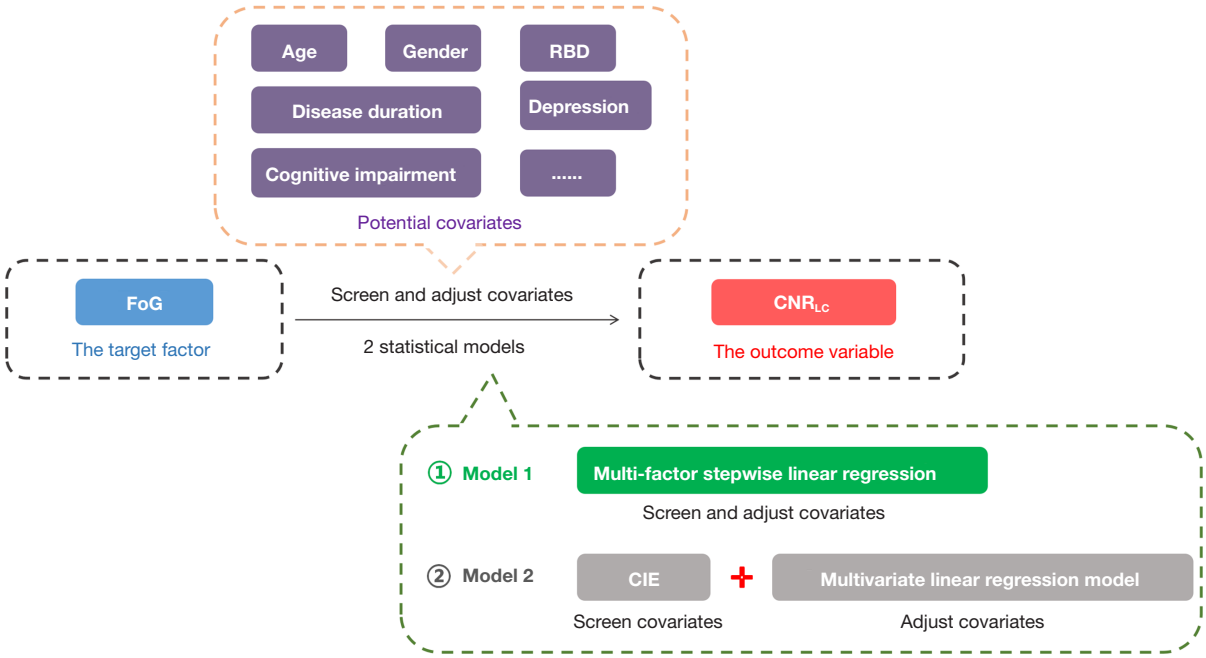

Figure 2 Flow diagram of the two statistical models. RBD, rapid-eye-movement sleep behavior disorder; FoG, freezing of gait; CNR_{LC}, CNR of the LC; CNR, contrast-to-noise ratio; LC, locus coeruleus; CIE, change-in-estimate.

LC circular regions of interest (ROIs) with the highest signal intensity (SI) at three consecutive levels from the inferior colliculus to the superior cerebellar peduncles while manually avoiding noise from the fourth ventricle (14,27). If the signal appeared ambiguous, ROIs were placed at the intended anatomical location of the LC.

The mean and standard deviation (SD) of the SI of the unilateral LC and medial pontine (PT) (as contrast area) in the same level image were measured. The above-described ROIs were outlined as indicated in *Figure 1C*. The same ROIs were applied to all participants, with an ROI size of 2 mm^2 for the LC and 30 mm^2 for the PT. The size of LC ROI was small due to its compact structure, consisting of approximately 5.4 voxels. The ROI size of LC was consistent with that of the majority of NM-MRI studies applying 2D sequences (14,15,27). We used the CNR of the LC (CNR_{LC}) to describe the signal characteristics of the LC. The equations for CNR_{LC} are as follows:

$$CNR_{LC} = \frac{SI_{LC} - SI_{PT}}{SD_{PT}} \quad [1]$$

where SI_{LC} is the mean SI of the unilateral LC ROIs; and SI_{PT} and SD_{PT} are the mean SI and the SD of PT ROIs, respectively.

Statistical analysis

All statistical analyses were calculated using SPSS 26.0 (IBM Corp, Armonk, NY, USA). P<0.05 was considered to indicate a statistically significant difference. Demographic and clinical data are described as the mean ± standard error (SE) or as the median and interquartile range (IQR) based on the characteristics of the data distribution. Correspondingly, two-sample *t*-tests, the Mann-Whitney test or Kruskal-Wallis test, and the χ^2 test were used for statistical analyses.

To clarify the relationship between FoG and LC degeneration, the CNR_{LC} in patients with PD was considered to be the outcome variable, and the FoG occurrence was considered to be the target factor. Finally, two statistical models were used to screen and adjust for covariates, as shown in *Figure 2*.

The multifactor stepwise linear regression model, model 1, included clinical data in with the statistical software automatically retaining the independent variable with the largest effect value.

For model 2, the confounders were screened using the CIE method; that is, after the addition or subtraction of variables, the independent variables that affected more than

Table 1 NM-MRI and clinical characteristics of the participants

Characteristics	PD (n=46)				HC (n=13)	P value
	PD FoG+ (n=22)	PD FoG– (n=24)	Total (n=46)	P value		
Left CNR_{LC}	2.84±0.21	3.54±0.15	3.20±0.14	0.009	4.12±0.27	0.003
Right CNR_{LC}	1.93±0.19	2.39±0.18	2.17±0.13	0.089	2.80±0.29	0.035
Age (years)	70.59±1.95	63.79±1.76	67.04±1.39	0.013	64.77±3.00	0.460
Gender (M/F)	13/9	14/10	27/19	0.958	8/5	0.854
FoG-Q	14.00 (3.50)	2.00 (3.00)	4.00 (12.00)	<0.001	–	–
Disease duration	7.09±0.50	3.11±0.36	5.02±0.42	<0.001	–	–
RBD (+/–)	15/7	11/13	26/20	0.127	–	–
MoCA	19.86±0.81	22.67±0.84	21.33±0.62	0.021	–	–
HAMD	20.00 (13.75)	12.50 (8.50)	16.00 (11.50)	0.002	–	–
AS	21.77±1.89	15.17±2.12	18.33±1.50	0.026	–	–
OH (+/–)	8/14	5/19	13/33	0.243	–	–
UPDRS-III (off)	76.36±3.44	42.75±3.62	58.83±3.52	<0.001	–	–

Data are presented as the mean ± SE, number, or median (IQR). NM-MRI, neuromelanin-sensitive magnetic resonance imaging; PD, Parkinson disease; FoG, freezing of gait; HC, healthy control; CNR_{LC}, CNR of the LC; CNR, contrast-to-noise ratio; LC, locus coeruleus; M, male; F, female; FoG-Q, Freezing of Gait Questionnaire; RBD, rapid-eye-movement sleep behavior disorder; MoCA, Montreal Cognitive Assessment; HAMD, Hamilton Depression Rating Scale; AS, Apathy Scale; OH, orthostatic hypotension; UPDRS-III, Unified Parkinson's Disease Rating Scale III; SE, standard error; IQR, interquartile range.

10% of the β values of the target factor in the initial model were retained (29). The multivariate linear regression model was then used to adjust for confounders.

We sought to eliminate collinearity variables to construct a stable data model, and the variance inflation factor (VIF) and correlation coefficient of all independent variables included in the model were calculated. The independent variables with VIF >2 and the correlation coefficient of two independent variables >0.7 were not included in the model as confounders (30).

Results

Comparison of NM-MRI features and clinical characteristics between the groups

We performed pairwise comparisons between the PD group and the HC group and between the PD FoG+ group and the PD FoG– group (*Table 1*). The results showed that the CNR of the left (P=0.003) and right LC (P=0.035) in patients with PD was significantly lower than that in HCs. In the comparison with that in the PD FoG– group, the CNR of the left LC was significantly decreased in the PD FoG+ group (P=0.009).

In terms of participants' clinical data, the PD FoG+ group, compared with the PD FoG– group, was older (P=0.013) and had a longer disease duration (P<0.001). In addition, the PD FoG + group had more severe nonmotor symptoms as indicated by significant differences in the nonmotor symptom scale, including HAMD score (P=0.002), AS score (P=0.026), UPDRS-III score (P<0.001), and MoCA score (P=0.021). There were no significant differences in the proportions of gender, RBD, or OH between the groups (P>0.05). The detailed NM-MRI and clinical characteristics of the groups are shown in *Table 1*.

Screening and adjustment of confounders

Since only the left CNR_{LC} was significantly different between the PD FoG– and PD FoG+ groups, we used the left CNR_{LC} as the outcome variable and the presence or absence of FoG as the target factor to examine their relationships in the two statistical models.

The independent variables that demonstrated the largest effect in model 1 were FoG, RBD, and gender. The CIE variables after screening in model 2 were age, RBD, MoCA

Table 2 β screened by the CIE method

Covariate	Basic model	Complete model
+/–	FoG	FoG
The initial regression coefficient of the covariate	0.169	0.111
Age (years)	0.152†	0.109
Gender	0.168	0.109
RBD	0.129†	0.129†
MoCA	0.141†	0.118
HAMD	0.193†	0.104
AS	0.163	0.108
OH	0.155	0.111
Disease duration	0.181	0.100
UPDRS-III (off)	0.106†	0.132†

†, indicates more than 10% change from the initial regression coefficient. CIE, change-in-estimate; FoG, freezing of gait; RBD, rapid-eye-movement sleep behavior disorder; MoCA, Montreal Cognitive Assessment; HAMD, Hamilton Depression Rating Scale; AS, Apathy Scale; OH, orthostatic hypotension; UPDRS-III, Unified Parkinson's Disease Rating Scale III.

Table 3 Multiple linear regression analysis of the factors influencing the left CNR_{LC}

Variables	β	95% CI	P
Model 1			
FoG	0.127	0.019, 0.236	0.023
RBD	0.182	0.073, 0.291	0.002
Gender	0.150	0.042, 0.257	0.007
Model 2			
FoG	0.153	0.019, 0.287	0.026
Age (years)	0.002	–0.006, 0.009	0.684
RBD	0.171	0.048, 0.294	0.008
MoCA	0.011	–0.006, 0.029	0.204
HAMD	0.005	–0.002, 0.012	0.148

Model 1, stepwise linear regression model. Model 2: linear regression model after screening for confounders via CIE method. CNR_{LC}, CNR of the LC; CNR, contrast-to-noise ratio; LC, locus coeruleus; CI, confidence interval; FoG, freezing of gait; RBD, rapid-eye-movement sleep behavior disorder; MoCA, Montreal Cognitive Assessment; HAMD, Hamilton Depression Rating Scale; CIE, change-in-estimate.

score, HAMD score, and UPDRS-III score (see *Table 2*). The UPDRS-III score was excluded from model 2 since it was collinear with FoG (the score had a VIF value of 2.392 and a correlation coefficient of –0.711, which met the definition of a collinear variable).

After adjustments were made for the abovementioned covariates, the two statistical models showed that FOG was an independent influencing factor for the outcome variable [model 1: β=0.127, 95% confidence interval (CI): 0.019–0.236, P=0.023; model 2: β=0.153, 95% CI: 0.019–0.287, P=0.026]. The other factors that could also independently associated with the outcome variable were RBD (model 1: β=0.182, 95% CI: 0.073–0.291, P=0.002; model 2: β=0.171, 95% CI: 0.048–0.294, P=0.008) and gender (model 1: β=0.150, 95% CI: 0.042–0.257, P=0.007). However, RBD demonstrated the greatest influence, followed by gender and FOG. The model results are shown in *Table 3*.

Discussion

In this study, after confounders were controlled for, it was found that the left CNR_{LC} in the FoG+ group was considerably lower than that in FoG– group, indicating that FoG in patients with PD is related to LC noradrenergic dysfunction. There may be several explanations for this relationship. First, the terminals of the noradrenergic neurons in the LC regulate the functional activities of dopaminergic neurons in multiple cortex regions (31,32). In line with this, FoG does not respond well to dopamine therapy, and animal models of PD suggest that LC NE deficiency might reduce the efficacy of levodopa therapy (33,34). Second, FoG is regarded as a disorder of advanced cortical activity (3,35) probably due to the decrease in LC noradrenergic neurons leading to a decrease in projections to the prefrontal cortex (36,37).

Our study revealed a statistically significant difference between the CNR of the left and right LC, with a notably higher CNR observed in the left LC. However, a previous postmortem study did not indicate there to be asymmetric distributions of NM in LC (38). Several NM-MRI studies have demonstrated a lateralized signal difference in the LC, and two potential explanations for this phenomenon may be considered. First, this lateralized signal difference in the LC is likely related to the heterogeneous signal distribution stemming from the high field strength and multichannel coils from different types of MRI scanners (39,40). For example, a higher contrast in the right LC was reported with Philips scanners, while a higher contrast in the left

LC was reported with the Siemens scanners (15,41), and similar results were obtained in our study using the Siemens scanner. Second, the signal on one side is often higher than that on the opposite side (the left side predominated in this study possibly due to the majority of participants being right-handed), and the LC also maintains synchronization of asymmetries throughout disease progression (42).

To investigate whether the FoG in patients with PD is an independent factor affecting the left CNR_{LC}, we comprehensively considered age, gender, cognitive impairment, depression, apathy, and OH symptoms in patients with PD, all of which have been reported to affect the signal characteristics of the LC (14-16,43-45). We examined disease duration and UPDRS-III score, which reflect disease severity and are also important factors associated with FoG in PD (46,47). They were all included in the regression model as potential confounders in this study. In model 2, UPDRS-III score was excluded as a collinearity variable. Its exclusion did not affect the reliability of the results since many studies have reported there to be no correlation between UPDRS-III score and LC degeneration (48,49).

In addition, a reduction in LC signal was observed to be more pronounced in PD patients with RBD than in those without RBD, and the LC signal in male patients was lower than that in female patients. We concluded that RBD and gender are also independent factors associated with the CNR values of the left LC. Consistent with the majority of related studies, RBD was accompanied by a significant reduction in the LC signal, owing to the extensive connection between the LC and brain and spinal cord in regulating arousal and autonomic function (50-53). As for the observed lower signal of the LC in males compared with that in females in patients with PD, we speculate this to be a result of the estrogen in females increasing the NM concentration in the LC target regions by promoting NE synthesis and reducing degradation (44).

In addition to the small sample size, our study involved two major limitations. First, The LC structure was not partitioned using manual segmentation. However, The LC structure has rostral, middle, and caudal functional subregions that project along distinct pathways to specific brain regions, thus exerting unique functions (9). Automated LC segmentation combined with the three-dimensional sequence-based template space may perform similarly to manual segmentation but involved a reduced workload, less subjectivity, and the ability to segment the LC along its full rostrocaudal extent (54,55). Second, one study has suggested that NE prodrugs are mostly effective in FoG in levodopa-resistant individuals (6). However, the FoG group was not divided into levodopa-resistant and nonresistant groups due to the small number of levodopa-resistant individuals in our study. In the future, we may garner further insights if we use automated segmentation to examine the regional and functional structure of the LC based on levodopa-resistant individuals.

In conclusion, NM-MRI provides a powerful tool for understanding the pathogenesis of FoG. Our study showed that the LC signal in the PD FoG+ group was lower than that in the PD FoG– group after confounders were controlled for, indicating that the FoG is related to LC noradrenergic dysfunction. In the future, NM-MRI may potentially become a novel biomarker for identifying individuals with FoG who respond well to NE prodrugs.

Acknowledgments

Funding: This work was supported by the Health and Technology Development Program of Jilin Province (No. 2021LC027).

Footnote

Reporting Checklist: The authors have completed the STROBE reporting checklist. Available at https://qims.amegroups.com/article/view/10.21037/qims-24-1486/rc

Conflicts of Interest: All authors have completed the ICMJE uniform disclosure form (available at https://qims.amegroups.com/article/view/10.21037/qims-24-1486/coif). The authors have no conflicts of interest to declare.

Ethical Statement: The authors are accountable for all aspects of the work in ensuring that questions related to the accuracy or integrity of any part of the work are appropriately investigated and resolved. This study was approved by the Ethics Review Committee of the China-Japan Union Hospital of Jilin University (No. 2023111003) and was conducted in accordance with the Declaration of Helsinki (as revised in 2013). Informed consent was obtained from all the patients.

References

1. Okuma Y, Silva de Lima AL, Fukae J, Bloem BR, Snijders AH. A prospective study of falls in relation to freezing of gait and response fluctuations in Parkinson's disease. Parkinsonism Relat Disord 2018;46:30-5.
2. O'Callaghan C, Hezemans FH, Ye R, Rua C, Jones PS, Murley AG, Holland N, Regenthal R, Tsvetanov KA, Wolpe N, Barker RA, Williams-Gray CH, Robbins TW, Passamonti L, Rowe JB. Locus coeruleus integrity and the effect of atomoxetine on response inhibition in Parkinson's disease. Brain 2021;144:2513-26.
3. Yan Y, Wang Z, Wei W, Yang Z, Guo L, Wang Z, Wei X. Correlation of brain iron deposition and freezing of gait in Parkinson's disease: a cross-sectional study. Quant Imaging Med Surg 2023;13:7961-72.
4. Hao H, Gao Z, Qin B. Research progress of freezing of gait. Chinese Journal of Neuroimmunology and Neurology 2018;25:375-8, 380.
5. Li Y, Wang L, Zhang Y. Research progress of executive dysfunction in Parkinson's disease. Chinese Journal of Geriatric Heart Brain and Vessel Diseases 2016;18:553-5.
6. Devos D, Defebvre L, Bordet R. Dopaminergic and non-dopaminergic pharmacological hypotheses for gait disorders in Parkinson's disease. Fundam Clin Pharmacol 2010;24:407-21.
7. Tohgi H, Abe T, Takahashi S, Takahashi J, Nozaki Y, Ueno M, Kikuchi T. Monoamine metabolism in the cerebrospinal fluid in Parkinson's disease: relationship to clinical symptoms and subsequent therapeutic outcomes. J Neural Transm Park Dis Dement Sect 1993;5:17-26.
8. Tohgi H, Abe T, Takahashi S, Ueno M, Nozaki Y. Cerebrospinal fluid dopamine, norepinephrine, and epinephrine concentrations in Parkinson's disease correlated with clinical symptoms. Adv Neurol 1990;53:277-82.
9. Bari BA, Chokshi V, Schmidt K. Locus coeruleus-norepinephrine: basic functions and insights into Parkinson's disease. Neural Regen Res 2020;15:1006-13.
10. Enochs WS, Petherick P, Bogdanova A, Mohr U, Weissleder R. Paramagnetic metal scavenging by melanin: MR imaging. Radiology 1997;204:417-23.
11. Cassidy CM, Zucca FA, Girgis RR, Baker SC, Weinstein JJ, Sharp ME, Bellei C, Valmadre A, Vanegas N, Kegeles LS, Brucato G, Kang UJ, Sulzer D, Zecca L, Abi-Dargham A, Horga G. Neuromelanin-sensitive MRI as a noninvasive proxy measure of dopamine function in the human brain. Proc Natl Acad Sci U S A 2019;116:5108-17.
12. Kitao S, Matsusue E, Fujii S, Miyoshi F, Kaminou T, Kato S, Ito H, Ogawa T. Correlation between pathology and neuromelanin MR imaging in Parkinson's disease and dementia with Lewy bodies. Neuroradiology 2013;55:947-53.
13. Mann DM. The locus coeruleus and its possible role in ageing and degenerative disease of the human central nervous system. Mech Ageing Dev 1983;23:73-94.
14. Li Y, Wang C, Wang J, Zhou Y, Ye F, Zhang Y, Cheng X, Huang Z, Liu K, Fei G, Zhong C, Zeng M, Jin L. Mild cognitive impairment in de novo Parkinson's disease: A neuromelanin MRI study in locus coeruleus. Mov Disord 2019;34:884-92.
15. Wang J, Li Y, Huang Z, Wan W, Zhang Y, Wang C, Cheng X, Ye F, Liu K, Fei G, Zeng M, Jin L. Neuromelanin-sensitive magnetic resonance imaging features of the substantia nigra and locus coeruleus in de novo Parkinson's disease and its phenotypes. Eur J Neurol 2018;25:949-e73.
16. Madelung CF, Meder D, Fuglsang SA, Marques MM, Boer VO, Madsen KH, Petersen ET, Hejl AM, Løkkegaard A, Siebner HR. Locus Coeruleus Shows a Spatial Pattern of Structural Disintegration in Parkinson's Disease. Mov Disord 2022;37:479-89.
17. Avanzino L, Lagravinese G, Abbruzzese G, Pelosin E. Relationships between gait and emotion in Parkinson's disease: A narrative review. Gait Posture 2018;65:57-64.
18. Wang X, Tian M, Zhang X, Liu Y. Research progress on the related factors of freezing of gait in Parkinson's disease. Journal of Internal Medicine Concepts & Practice 2022;17:339-43.
19. Postuma RB, Berg D, Stern M, Poewe W, Olanow CW, Oertel W, Obeso J, Marek K, Litvan I, Lang AE, Halliday G, Goetz CG, Gasser T, Dubois B, Chan P, Bloem BR, Adler CH, Deuschl G. MDS clinical diagnostic criteria for Parkinson's disease. Mov Disord 2015;30:1591-601.
20. Giladi N, Shabtai H, Simon ES, Biran S, Tal J, Korczyn AD. Construction of freezing of gait questionnaire for patients with Parkinsonism. Parkinsonism Relat Disord 2000;6:165-70.
21. Stiasny-Kolster K, Mayer G, Schäfer S, Möller JC, Heinzel-Gutenbrunner M, Oertel WH. The REM sleep behavior disorder screening questionnaire--a new

diagnostic instrument. Mov Disord 2007;22:2386-93.
22. Wang Y, Wang ZW, Yang YC, Wu HJ, Zhao HY, Zhao ZX. Validation of the rapid eye movement sleep behavior disorder screening questionnaire in China. J Clin Neurosci 2015;22:1420-4.
23. Nasreddine ZS, Phillips NA, Bédirian V, Charbonneau S, Whitehead V, Collin I, Cummings JL, Chertkow H. The Montreal Cognitive Assessment, MoCA: a brief screening tool for mild cognitive impairment. J Am Geriatr Soc 2005;53:695-9.
24. Romera I, Pérez V, Menchón JM, Polavieja P, Gilaberte I. Optimal cutoff point of the Hamilton Rating Scale for Depression according to normal levels of social and occupational functioning. Psychiatry Res 2011;186:133-7.
25. Leentjens AF, Dujardin K, Marsh L, Martinez-Martin P, Richard IH, Starkstein SE, Weintraub D, Sampaio C, Poewe W, Rascol O, Stebbins GT, Goetz CG. Apathy and anhedonia rating scales in Parkinson's disease: critique and recommendations. Mov Disord 2008;23:2004-14.
26. Goetz CG, Fahn S, Martinez-Martin P, Poewe W, Sampaio C, Stebbins GT, et al. Movement Disorder Society-sponsored revision of the Unified Parkinson's Disease Rating Scale (MDS-UPDRS): Process, format, and clinimetric testing plan. Mov Disord 2007;22:41-7.
27. Zhou C, Guo T, Wu J, Wang L, Bai X, Gao T, Guan X, Gu L, Huang P, Xuan M, Gu Q, Xu X, Zhang B, Cheng W, Feng J, Zhang M. Locus Coeruleus Degeneration Correlated with Levodopa Resistance in Parkinson's Disease: A Retrospective Analysis. J Parkinsons Dis 2021;11:1631-40.
28. Fernandes P, Regala J, Correia F, Gonçalves-Ferreira AJ. The human locus coeruleus 3-D stereotactic anatomy. Surg Radiol Anat 2012;34:879-85.
29. Weng HY, Hsueh YH, Messam LL, Hertz-Picciotto I. Methods of covariate selection: directed acyclic graphs and the change-in-estimate procedure. Am J Epidemiol 2009;169:1182-90.
30. Vatcheva KP, Lee M, McCormick JB, Rahbar MH. Multicollinearity in Regression Analyses Conducted in Epidemiologic Studies. Epidemiology (Sunnyvale) 2016.
31. Ponzio F, Hallman H, Jonsson G. Noradrenaline and dopamine interaction in rat brain during development. Med Biol 1981;59:161-9.
32. Benarroch EE. Locus coeruleus. Cell Tissue Res 2018;373:221-32.
33. Ferrucci M, Gesi M, Lenzi P, Soldani P, Ruffoli R, Pellegrini A, Ruggieri S, Paparelli A, Fornai F. Noradrenergic loss enhances MDMA toxicity and induces ubiquitin-positive striatal whorls. Neurol Sci 2002;23 Suppl 2:S75-6.
34. Archer T, Fredriksson A. Influence of noradrenaline denervation on MPTP-induced deficits in mice. J Neural Transm (Vienna) 2006;113:1119-29.
35. Wang L, Gan C, Sun H, Ji M, Zhang H, Cao X, Wang M, Yuan Y, Zhang K. Impaired structural and reserved functional topological organizations of brain networks in Parkinson's disease with freezing of gait. Quant Imaging Med Surg 2023;13:66-79.
36. Barbeau H, Rossignol S. Initiation and modulation of the locomotor pattern in the adult chronic spinal cat by noradrenergic, serotonergic and dopaminergic drugs. Brain Res 1991;546:250-60.
37. Espay AJ, LeWitt PA, Kaufmann H. Norepinephrine deficiency in Parkinson's disease: the case for noradrenergic enhancement. Mov Disord 2014;29:1710-9.
38. German DC, Walker BS, Manaye K, Smith WK, Woodward DJ, North AJ. The human locus coeruleus: computer reconstruction of cellular distribution. J Neurosci 1988;8:1776-88.
39. Betts MJ, Cardenas-Blanco A, Kanowski M, Jessen F, Düzel E. In vivo MRI assessment of the human locus coeruleus along its rostrocaudal extent in young and older adults. Neuroimage 2017;163:150-9.
40. Tona KD, Keuken MC, de Rover M, Lakke E, Forstmann BU, Nieuwenhuis S, van Osch MJP. In vivo visualization of the locus coeruleus in humans: quantifying the test-retest reliability. Brain Struct Funct 2017;222:4203-17.
41. Clewett DV, Lee TH, Greening S, Ponzio A, Margalit E, Mather M. Neuromelanin marks the spot: identifying a locus coeruleus biomarker of cognitive reserve in healthy aging. Neurobiol Aging 2016;37:117-26.
42. Liu Q, Wang P, Liu C, Xue F, Wang Q, Chen Y, Hou R, Chen T. An investigation of neuromelanin distribution in substantia nigra and locus coeruleus in patients with Parkinson's disease using neuromelanin-sensitive MRI. BMC Neurol 2023;23:301.
43. Shibata E, Sasaki M, Tohyama K, Kanbara Y, Otsuka K, Ehara S, Sakai A. Age-related changes in locus ceruleus on neuromelanin magnetic resonance imaging at 3 Tesla. Magn Reson Med Sci 2006;5:197-200.
44. Bangasser DA, Wiersielis KR, Khantsis S. Sex differences in the locus coeruleus-norepinephrine system and its regulation by stress. Brain Res 2016;1641:177-88.
45. Matzaras R, Shi K, Artemiadis A, Zis P, Hadjigeorgiou G, Rominger A, Bassetti CLA, Bargiotas P. Brain Neuroimaging of Rapid Eye Movement Sleep Behavior

Disorder in Parkinson's Disease: A Systematic Review. J Parkinsons Dis 2022;12:69-83.
46. Matsuura K, Maeda M, Tabei KI, Umino M, Kajikawa H, Satoh M, Kida H, Tomimoto H. A longitudinal study of neuromelanin-sensitive magnetic resonance imaging in Parkinson's disease. Neurosci Lett 2016;633:112-7.
47. Prasuhn J, Prasuhn M, Fellbrich A, Strautz R, Lemmer F, Dreischmeier S, Kasten M, Münte TF, Hanssen H, Heldmann M, Brüggemann N. Association of Locus Coeruleus and Substantia Nigra Pathology With Cognitive and Motor Functions in Patients With Parkinson Disease. Neurology 2021;97:e1007-16.
48. Ge HL, Chen XY, Lin YX, Ge TJ, Yu LH, Lin ZY, Wu XY, Kang DZ, Ding CY. The prevalence of freezing of gait in Parkinson's disease and in patients with different disease durations and severities. Chin Neurosurg J 2020;6:17.
49. Mills KA, Mari Z, Bakker C, Johnson V, Pontone GM, Pantelyat A, Troncoso JC, Pletnikova O, Dawson TM, Rosenthal LS. Gait function and locus coeruleus Lewy body pathology in 51 Parkinson's disease patients. Parkinsonism Relat Disord 2016;33:102-6.
50. Nobileau A, Gaurav R, Chougar L, Faucher A, Valabrègue R, Mangone G, Leu-Semenescu S, Lejeune FX, Corvol JC, Arnulf I, Vidailhet M, Grabli D, Degos B, Lehéricy S. Neuromelanin-Sensitive Magnetic Resonance Imaging Changes in the Locus Coeruleus/Subcoeruleus Complex in Patients with Typical and Atypical Parkinsonism. Mov Disord 2023;38:479-84.
51. Boeve BF, St Louis EK, Kantarci K. Neuromelanin-sensitive imaging in patients with idiopathic rapid eye movement sleep behaviour disorder. Brain 2016;139:1005-7.
52. Ehrminger M, Latimier A, Pyatigorskaya N, Garcia-Lorenzo D, Leu-Semenescu S, Vidailhet M, Lehericy S, Arnulf I. The coeruleus/subcoeruleus complex in idiopathic rapid eye movement sleep behaviour disorder. Brain 2016;139:1180-8.
53. Samuels ER, Szabadi E. Functional neuroanatomy of the noradrenergic locus coeruleus: its roles in the regulation of arousal and autonomic function part I: principles of functional organisation. Curr Neuropharmacol 2008;6:235-53.
54. Liu KY, Acosta-Cabronero J, Cardenas-Blanco A, Loane C, Berry AJ, Betts MJ, Kievit RA, Henson RN, Düzel E; Howard R, Hämmerer D. In vivo visualization of age-related differences in the locus coeruleus. Neurobiol Aging 2019;74:101-11.
55. Sibahi A, Gandhi R, Al-Haddad R, Therriault J, Pascoal T, Chamoun M, Boutin-Miller K, Tardif C, Rosa-Neto P, Cassidy CM. Characterization of an automated method to segment the human locus coeruleus. Hum Brain Mapp 2023;44:3913-25.

Cite this article as: Yang Y, Zhang M, Yan Y, Chang Y, Chen M. Relationship between freezing of gait in Parkinson disease and locus coeruleus dysfunction: a neuromelanin-sensitive magnetic resonance imaging study. Quant Imaging Med Surg 2025;15(1):911-920. doi: 10.21037/qims-24-1486